An introduction to Dynamical Mean Field Theory (DMFT) and DFT+DMFT

B. Amadon
CEA, DAM, DIF, F-91297 Arpajon, France

International summer School in electronic structure Theory: electron correlation in Physics and Chemistry (ISTPC), June 2017

Contents

In these notes, I present a brief introduction to strong correlations in solid state physics, to Dynamical Mean Field Theory (DMFT) and to the combination of Density Functional Theory (DFT) and DMFT (See also references [1], [2], and [3]).

1 Introduction to strong correlation: localized orbitals

1.1 Atomic orbitals

We first focus on the spatial localization of orbitals as a function of their principal quantum numbers: $1s$, $2p$ and $3d$ and $4f$ orbitals are orthogonal to lower orbitals only through the angular part because for their value of l, they are the orbitals with the lowest principal quantum number[3]. As a consequence,

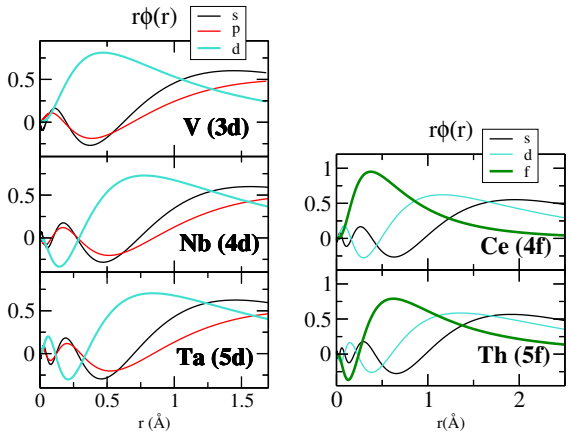

Figure 1: Radial part of valence wavefunctions of some atoms (computed in DFT/LDA).

the radial part of the wavefunction is not constrained by orthogonality, and can lower its Coulomb interaction with the nucleus by being more localized. Thus, these orbitals are more localized than others. Fig. 1 illustrates the localization of $3d$ and $4f$ with respect to $4d$, $5d$ and $5f$ orbitals. Indeed, transition metals and lanthanides are notorious examples of systems exhibiting strong correlation effects.

Concerning the angular part, it has more and more nodal planes as l increases, thus in particular, d and f orbitals are fairly localized in space. As a consequence, $4d$, $5d$ and $5f$ orbitals exhibit also important correlation effects.

1.2 Localization or delocalization of electrons?

Two main consequences arise from the localization of orbitals:

- When a solid is formed from atoms, the overlap of localized orbitals is weaker than for delocalized orbitals and thus the bandwidth W is smaller (see Fig. 2).
- The more localized are the orbitals, the stronger the local interactions "U" between electrons are, because electrons are closer to each other.

The simplest example to illustrate these two effects is the formation of the H_2 molecule. In this case, this competition between chemical bonding and interaction leads to a change of the ground state

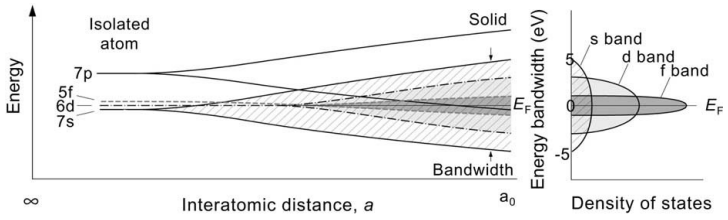

Figure 2: Schematic bandwidth from some orbitals as a function of pressure: the more localized are the orbitals, the smaller is the bandwidth (from [4]).

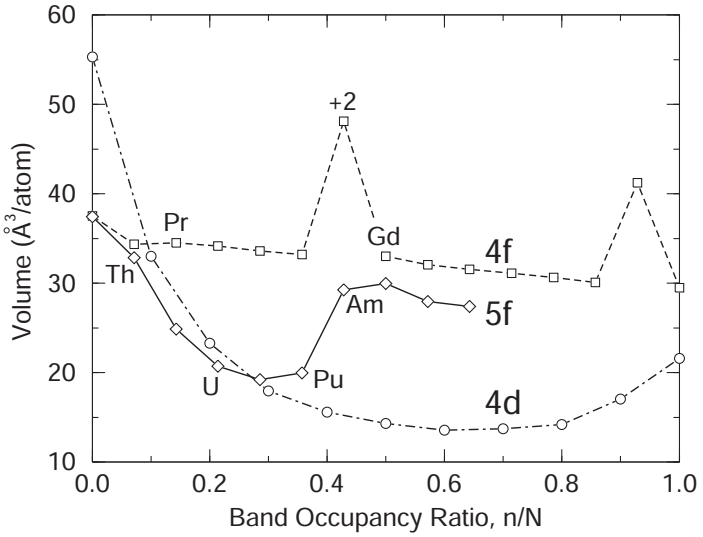

Figure 3: Evolution of volume of pure elements are a function of volume for some lines of the periodic table (from [5]).

as the interatomic distance increases. At large distance, the electrons are localized each on its atom to avoid the Coulomb interaction with the other electrons (here $U > W$). At small distance, the two electrons delocalize in a bonding molecular orbital.

Let's see another consequence of this for solids on Fig. 3. It represents the evolution of volume of pure elements as a function of the number of electrons, for $4d$, $4f$ and $5f$ elements. We now discuss each curve:

- $4d$ orbitals are fairly delocalized, and form bands. Thus, as Z increases, electrons fill the $4d$ band. First the bonding states are filled and then antibonding states. As a consequence, the volume decreases and then increases. This experimental observation is thus coherent with the delocalization of $4d$ electrons.

- For lanthanides, $4f$ electrons are localized, thus there is a negligible overlap between $4f$ orbitals. As a consequence, adding electrons inside the f bands has no effect on the cohesion of the cristal.

- Actinides: The localization appears at the middle of the serie. As Z increases, the $5f$ orbitals are more and more localized because of the attraction with the nucleus. In the middle of the series, the system choose to localize electrons to lower the energy.

2 The Hubbard model

In this section, we will study the Hubbard model, which is appropriate to study the localisation/delocalisation competition.

From the lecture of Emmanuel Fromager on second quantization, one can write the Hamiltonian as

$$H = \sum_i \langle i|h|j\rangle c_i^\dagger c_j + \sum_{i,j,k,l} \langle ij|v|kl\rangle c_i^\dagger c_j^\dagger c_k c_l \tag{1}$$

In this equation, i, j, k, l belongs to a complete one particle basis. If (1) the sums in this equation are restricted to only one orbital per atoms, (2) only on site interactions are kept, one can show that one recover the Hubbard model.

Exercice: Show how this expression reduces to the Hubbard model if the preceding conditions are fulfilled.

The Hubbard model writes:

$$H = \sum_{i \neq j} t_{ij} c_i^\dagger c_j + \sum_i \epsilon_0 (n_{i\uparrow} + n_{i\uparrow}) + \sum_i U n_{i\uparrow} n_{i\downarrow} \tag{2}$$

In this equation, as we have only one orbital per site, i, j refers to atomic sites. We will now try to understand two limits of this Hamiltonian.

2.1 Delocalization limit: $U/t << 1$

Let's suppose that we can neglect the interaction term.

$$H = \sum_{j \neq i} t_{ij} c_i^\dagger c_j + \epsilon_0 (n_{i\uparrow} + n_{i\downarrow}) \tag{3}$$

In this case, one can easily solve this non interacting Hamiltonian either by direct diagonalisation or by using Bloch states: We can define Bloch states $|k\rangle$ as

$$|k\rangle = \frac{1}{\sqrt{N}} \sum_i |T_i\rangle \mathrm{e}^{ikT_i} \tag{4}$$

where $|T_i\rangle$ are atomic orbitals: $\langle r|T_i\rangle = \phi(r - T_i)$ on site i. We also have

$$|T_i\rangle = \frac{1}{\sqrt{N}} \sum_k |k\rangle \mathrm{e}^{-ikT_i} \tag{5}$$

We also have the change of basis for creation and annihilation operators:

$$c_i^\dagger = \frac{1}{\sqrt{N}} \sum_k c_k^\dagger \mathrm{e}^{-ikT_i} \tag{6}$$

$$c_i = \frac{1}{\sqrt{N}} \sum_k c_k \mathrm{e}^{ikT_i} \tag{7}$$

As a consequence, one can show (do it in Exercice) that:

$$H = \sum_k \epsilon_k c_k^\dagger c_k \tag{8}$$

with $\epsilon_k = \frac{1}{N} \sum_{ij} t_{ij} \mathrm{e}^{-ik(T_i - T_j)}$

Figure 4: For $U/t >> 1$, the cost of a hopping is $E(|\uparrow\downarrow\rangle) + E(|0\rangle) - 2E(|\uparrow\rangle) = U$

Let now suppose that we are in one dimension, and t_{ij} is non zero only for neighboring atoms, in this case, we have (note that t is negative) the following dispersion relation which gives the energy of levels as a function of the value of k.

$$\epsilon_k = \epsilon_0 + 2t\cos(ka) \tag{9}$$

According to Bloch theorem, k must belong to the first Brillouin Zone $[-\frac{\pi}{a}, \frac{\pi}{a}]$, where a is the distance between atoms. We now suppose that we have one electron per atom, whereas there are two states per atoms. As a consequence, the band is half filled. The system is thus metallic and the Fermi levels is at ϵ_0.

2.2 Localization limit: $U/t >> 1$

$$H = \sum_i U n_{i\uparrow} n_{i\uparrow} + \sum_i \epsilon_0 (n_{i\uparrow} + n_{i\downarrow}) \tag{10}$$

In this case, the Hamiltonian is a sum of Hamiltonians for independent atoms ! We thus have to solve the atomic problem.

The size of the Hilbert space for this system is four (2^2):

- 0 electron: $|0\rangle$:$E = 0$
- 1 electron: $|\uparrow\rangle$ and $|\downarrow\rangle$: $E = \epsilon_0$
- 2 electrons: $|\uparrow\downarrow\rangle$: $E = 2\epsilon_0 + U$

Let us now suppose that the system as one electron per atom. From the above energies, one can compute the cost associated to the hopping of one electron from one atom to another atom (see Fig. 4). The cost is U. The order of magnitude of U in a real system is a few eV. As a consequence, at room temperature, electrons will be localized and the system is called a Mott insulator. The insulating character comes from interactions and not from a band structure effect.

One can also compute the photoemission spectra, ie the energy to add ($E(|\uparrow\downarrow\rangle) - E(|\uparrow\rangle) = \epsilon_0 + U$) or remove ($E(|\uparrow\rangle) - E(|0\rangle) = \epsilon_0$) an electron. We see that the photoemission spectra (or spectral function) will have two peaks located at ϵ_0 and $\epsilon_0 + U$. The two peaks are separated by U which is thus the photoemission gap. These peaks are called Hubbard bands.

2.3 The Mott transition

From these two limits, one can deduce that as U/t will increase, the systems will change from a metal to a Mott insulator. This is the phenomenon of the Mott transition. But we need an approximation to find the solution for intermediate values of U/t.

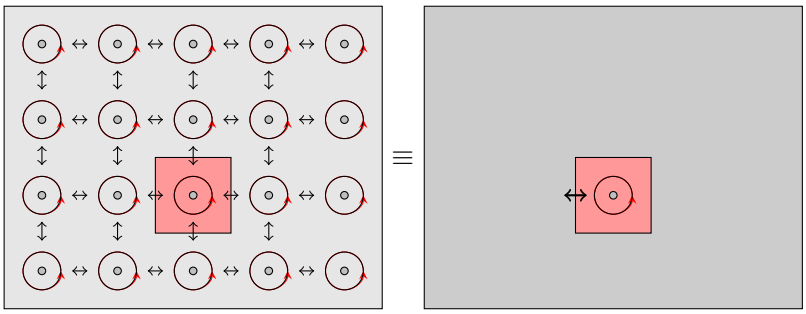

Figure 5: The first DMFT idea: The Hubbard model physics can be mimicked by an Anderson model

3 The Dynamical Mean Field Theory

3.1 The Anderson model

We would like to describe correctly the on-site Coulomb interactions which are essential to describe correctly the atomic limit. The first idea of DMFT is to mimic the Hubbard model by a correlated atom with the exact Coulomb interaction, embedded in a bath of uncorrelated orbitals (see Fig. 5). The effect of all the other atoms are gathered in the bath. This is a Anderson model[6] whose Hamiltonian writes:

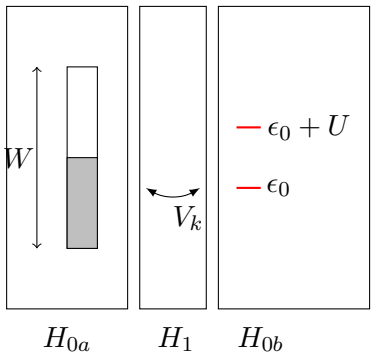

$$H_{\text{Anderson}} = \underbrace{\sum \omega_k a^+_{k,\sigma} a_{k\sigma}}_{H_{0a}} + \underbrace{\sum_{k,\sigma} V_k (a^+_{k,\sigma} c_\sigma + c^+_\sigma a_{k,\sigma})}_{H_1} + \underbrace{\epsilon_0 (n_\uparrow + n_\downarrow) + U n_\uparrow n_\downarrow}_{H_{0b}}$$

This is a mean field idea. However, we do not have only one electron in an effective field as in usual static mean field theory, but a whole many body atom whose interactions will be described exactly. Moreover the Anderson model will be defined self-consistently, but we will discuss this in the next section. We just focus in this section on the physics of the Anderson model. Once again, we are going to investigate several limiting cases for this Hamiltonian

3.1.1 The isolated atom limit: $V_k = 0$

This case is identical to the limit $U/t >> 1$ of the Hubbard model: the correlated atom is insulating.

3.1.2 The $U = 0$ limit

The hamiltonian writes:

$$H_{\text{Anderson}} = \sum \omega_k a^+_{k,\sigma} a_{k\sigma} + \sum_{k,\sigma} V_k (a^+_{k,\sigma} c_\sigma + c^+_\sigma a_{k,\sigma}) + \epsilon_0 (n_\uparrow + n_\downarrow)$$

This is again a non interacting system which can be solved easily: The atomic level will hybridize with the levels at ω_k, and will acquire a width.

Let's compute the Green's function of this system. We can use the equation of motion of the (non interacting) Green's function presented in the lecture of Fabien Bruneval, we thus have:

$$(\omega I - H)G = I \tag{11}$$

The dimension of these matrices is equal to N+1. It contains the N uncorrelated orbitals ω_k and the correlated orbital ϵ_0. The diagonal elements of H are the energies ω_k and ϵ_0. The only off diagonal terms are the coupling elements of the level at ϵ_0 to the levels at ω_k.

$$\begin{pmatrix} \epsilon_0 & V_1 & ... & V_k & ... & V_N \\ V_1 & \omega_1 & 0 & 0 & 0 & 0 \\ .... & 0 & ..... & 0 & 0 & 0 \\ V_k & 0 & 0 & \omega_k & 0 & 0 \\ ... & 0 & 0 & 0 & ..... & 0 \\ V_N & 0 & 0 & 0 & 0 & \omega_N \end{pmatrix}$$

$$G = (\omega I - H)^{-1} \tag{12}$$

We can easily inverse this matrix and compute the Green's function of the correlated orbital

Exercice: Use the formula $A^{-1} = \mathrm{Com}(A)^T/\mathrm{det}A$ to compute the correlated level Green's function. We obtain:

$$G(\omega) = \frac{1}{\omega - \epsilon_0 - \sum_k \frac{V_k^2}{\omega - \omega_k}} \tag{13}$$

We now define the Hybridization function $\Delta(\omega)$ as:

$$\Delta(\omega) = \sum_k \frac{V_k^2}{\omega - \omega_k} \tag{14}$$

We can now compute the spectral function of this system by computing (see lecture of Xavier Blase):

$$A(\omega) = -\frac{1}{\pi}\mathrm{Im}G^R(\omega + i\delta) \tag{15}$$

We need[1]

$$\Delta(\omega + i\delta) = \sum_k \frac{V_k^2}{\omega - \omega_k} - i\pi \sum_k |V_k|^2 \delta(\omega - \omega_k) \tag{16}$$

If $\Delta = 0$, then the spectral function has a peak at ϵ_0. Using the last two equations, the peak at ϵ_0 in the spectral function will be shifted by the real part of Δ and will be broadened by the imaginary part of Δ. Interesting, the imaginary part of Δ recovers the Fermi golden rule (width of the level coupled to the continuum is $\pi \sum_k |V_k|^2 \delta(\omega - \omega_k)$).

3.1.3 The Anderson Molecule

We now simplify the bath by replacing it by a single level. We reproduce here the exemple detailed in Ref. [7].

We suppose that U is infinite so the double occupation of the localized level is impossible. Finally we limit our study to the states with 2 electrons. With these constraints, we have 5 possible states in the Hilbert space: the first is the double occupation of the bath level (this is a state with S=0) and

[1] We use $\lim_{\delta\to 0} \frac{1}{\pi} \frac{\delta}{x^2+\delta^2} = \delta(x)$.

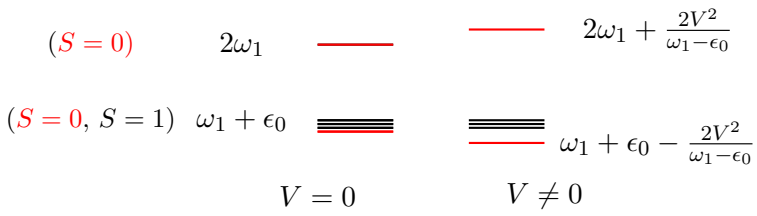

Figure 6: Two electrons levels with $V = 0$ and V small

there are four states with one electron in the bath level and one electron in the localized level. Among these four states, there are one triplet (S=1) and one singulet (S=0). If $V = 0$, then the four levels are degenerated. On Fig. 6, the singlet states are in red.

If the hybridization V is non zero, then the two states with $S = 0$ couple (see Fig. 6). As a consequence we have a possible transition between the singlet and the triplet state at very low energy. This phenomenon has the same physical origin as the Kondo effect. It shows that a resonance exists even in a very strongly correlated system (U is large) and this resonance will be at the Fermi level. We can define a temperature T^* corresponding to the difference of energy between the singlet and triplet state. Below this temperature, the system will exhibit the resonance, which will fade as temperature increases. Moreover, below this temperature, the magnetic moment of the localized level is completely cancelled by the formation of the singlet state.

Exercice: Compute the stabilization energy indicated in Fig 6. To do this, either you compute the eigenfunctions of the spin operators for S=0 and then you diagonalise a matrix of dimension 2 (see Ref.[7]). Or you can use the second quantization and write the variational wave function for the singlet as $|\Psi\rangle = (a_0 + a_1(c^\dagger_{0\uparrow}a_{1\uparrow} + c^\dagger_{0\downarrow}a_{1\downarrow}))|\Phi_0\rangle$ where $\Phi_0\rangle$ is a ground state with the orbital at ω_1 completely filled and solve the Schrödinger equation of our simple model for this variational wave function. It can be generalized to a large number of bath orbitals (see the discussion in Ref. [7]). Compare the stabilization energies in the two cases.

3.2 The self consistency condition and the DMFT loop

Following the definition of the Green's function on the local orbital basis

$$G_{ij}(t) = -i\langle N|T(c_i^\dagger(t)c_j(0)|N\rangle \tag{17}$$

one can compute the Bloch Green's function

$$G_{\mathbf{k}}(t) = \frac{1}{N}\sum_{ij} \mathrm{e}^{i\mathbf{k}(T_i - T_j)} G_{ij}(t) \tag{18}$$

thus, in frequency

$$G_{\mathbf{k}}(\omega) = \frac{1}{N}\sum_{ij} \mathrm{e}^{i\mathbf{k}(T_i - T_j)} G_{ij}(\omega) \tag{19}$$

Using the equation of Motion of the Green's function $(\omega - H - \Sigma)G = 1$, the lattice Green's function for the Hubbard model is written:

$$G_{\mathbf{k}}(\omega) = \frac{1}{\omega - \epsilon_{\mathbf{k}} - \Sigma_{\mathbf{k}}(\omega)} \tag{20}$$

where the self energy is unknown. The local Green's function of the lattice is

$$G_{ii}(\omega) = \frac{1}{N}\sum_{\mathbf{k}} \mathrm{e}^{ik(T_i - T_i)} G_{\mathbf{k}}(\omega) = \frac{1}{N}\sum_{\mathbf{k}} G_{\mathbf{k}}(\omega) \tag{21}$$

Besides, the Green's function for the Anderson impurity model is

$$G_{\text{Anderson}}(\omega) = \frac{1}{\omega - \epsilon_0 - \Delta(\omega) - \Sigma(\omega)} \tag{22}$$

The DMFT idea is to identify the local Green's function of the Hubbard model with the Green's function of Anderson model and the self energy of the Hubbard model to be equal to the self energy of the Anderson model [2] : it is the **self-consistency relation** of DMFT. This implies in particular that the local one particle excitations of the Hubbard model will be the same as the one particle excitations of the Anderson model. This writes:

$$\frac{1}{N}\sum_k \frac{1}{\omega - \epsilon_{\mathbf{k}} - \Sigma(\omega)} = \frac{1}{\omega - \epsilon_0 - \Delta(\omega) - \Sigma(\omega)} \tag{27}$$

This equation enables us to find $\Delta(\omega)$ as a function of the self energy: $\Delta = \Delta[\Sigma]$ and also $\epsilon_0 = \frac{1}{N}\sum_{\mathbf{k}} {\epsilon_{\mathbf{k}}}^3$

Besides, the solution of the Anderson model enables us to have the self energy from the value of ϵ_0 and Δ.[4] So this creates a system of two equations that can be solved self-consistently. These two equations constitute the DMFT self-consistent loop that can be solved by iteration.

3.3 The Hubbard model in DMFT

The main results for the Hubbard model phase diagram in DMFT (without magnetism and for one electron per atom) are sum up on Figs. 7 and 8. First, the metal insulator is a first order phase transition. Moreover, the paramagnetic insulating phase with a degeneracy of two can be described in contrary to the static mean field approximation which breaks the symmetry and creates magnetism.

Let's describe the evolution of the spectral function. At large value of U, the Hubbard bands are present but still broadened by hybridization. Then, a resonance peak appears at the Fermi level and grows, as U/t decreases. Importantly thus, the metallic phase appears whereas the Hubbard band are still present in the photoemission spectra. Such feature is also not described by the static mean field approximation. Let us finally outline that in DMFT, both the atomic limit ($U/t >> 1$) and the delocalization limit ($U/t << 1$) are exact.

4 DFT+DMFT

The main idea of DFT+DMFT is to use the DFT/LDA Hamiltonian to define the one body term of the Hubbard model and then supplement it by an exact Coulomb interaction for the correlated orbital

[2] Thus we have expressed also the self energy in the Bloch basis. We start from the expression of the self energy as a sum of local self energies on different sites:

$$\Sigma = \sum_{T_i} |T_i\rangle \Sigma(\omega) \langle T_i| \tag{23}$$

We use then

$$|T_i\rangle = \frac{1}{\sqrt{N}} \sum_{\mathbf{k}} |\mathbf{k}\rangle \mathrm{e}^{-i\mathbf{k}T_i} \tag{24}$$

Thus by replacing the last equation in Eq. 23, we have (do the derivation in exercice).

$$\Sigma = \sum_{\mathbf{k}} |\mathbf{k}\rangle \Sigma(\omega) \langle \mathbf{k}'| \tag{25}$$

Thus

$$\langle \mathbf{k}|\Sigma|\mathbf{k}\rangle = \Sigma(\omega) \tag{26}$$

Thus for a local self-energy, the self energy in the basis of Bloch states is equal to the local self-energy.

[3] Equivalently, one can say that the non interacting Green's function $\mathcal{G}_0^{-1} = \omega - \epsilon_0 - \Delta(\omega)$ can be obtained from the self-energy.

[4] Equivalently, one can obtain the Green's function and the self energy of the Anderson model as a function of the non interacting Green's function

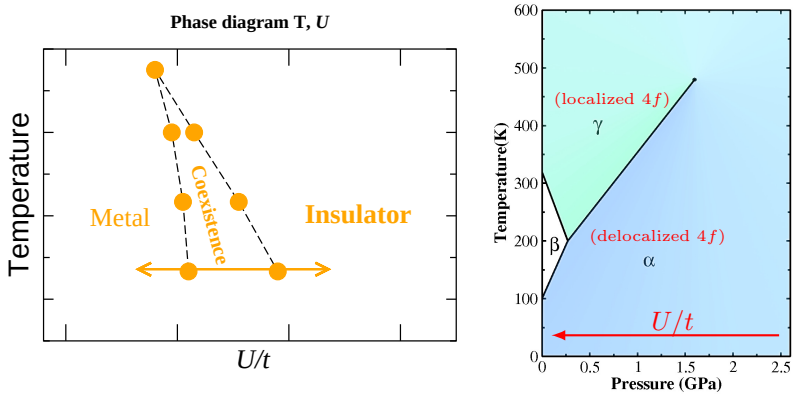

Figure 7: Phase diagram of the Hubbard model in DMFT compared to phase diagram of Cerium.

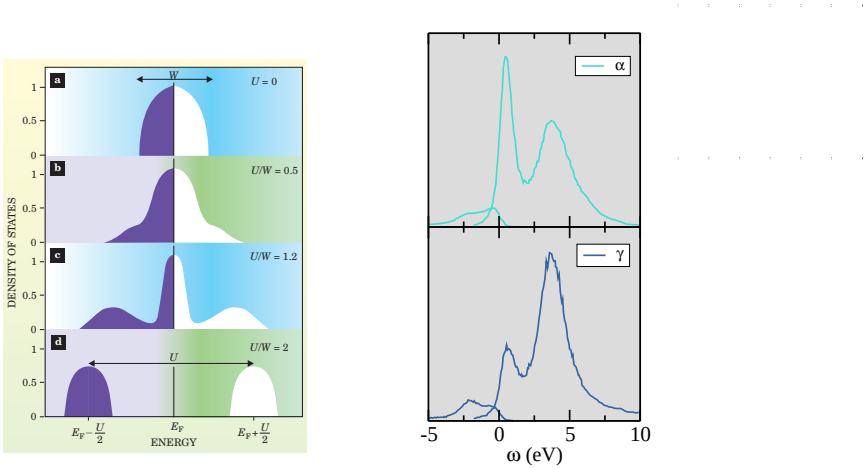

[G.Kotliar *et al* Phys. Today, AIP, 57, 53-59 (2004)]

[E. Weschke, *et al* Phys. Rev. B 44, 8304 (1991)
M. Grioni, *et al* Phys. Rev. B 55, 2056 (1997)]

Figure 8: Evolution of the spectral function in the Hubbard model (from Ref[8]) compared to spectral function in cerium.

subset.

However, to apply DMFT ideas to a real system, one need first to define correlated orbitals[9, 10, 11] and a corresponding value of the effective interaction U[12]. This is important and is discussed in the first subsection. I just outline here that there is no unique way to define correlated orbitals. So several choices have been made in the litterature. It includes atomic orbitals, or wannier orbitals. When the choice of correlated orbitals is done, the effective interaction for these orbitals has to be computed. The most used formalism is the constrained Random Phase Approximation method[12] which considers that the effective interaction between correlated electrons is the bare interaction screened by all the non correlated electrons. It thus requires the calculation of a non interacting polarisability and the inverse dielectric function as presented in the lectures of Fabien Bruneval, and Francesco Sottile. It is described in the second subsection.

Then, using correlated orbitals and related values of U, a DFT+DMFT calculation can be carried out.

4.1 Correlated orbitals: how to define them ?

4.1.1 Projected Local Orbitals Wannier functions and Maximally localized Wannier functions.

Projected Wannier functions are defined in Refs. [9, 11]. We first introduce the auxiliary wavefunctions $|\tilde{\chi}^{\mathbf{R}}_{\mathbf{k}m}\rangle$ as

$$|\tilde{\chi}^{\mathbf{R}}_{\mathbf{k}m}\rangle \equiv \sum_{\nu\in\mathcal{W}} |\Psi^{\sigma}_{\mathbf{k}\nu}\rangle\langle\Psi^{\sigma}_{\mathbf{k}\nu}|\chi^{\mathbf{R}}_{\mathbf{k}m}\rangle. \tag{28}$$

For a given atomic site $\mathbf{R}$, we call $|\chi^{\mathbf{R}}_{\mathbf{k}m}\rangle$ the Bloch transform of isolated atomic orbitals with projected angular momentum m. $|\Psi^{\sigma}_{\mathbf{k}\nu}\rangle$ are Kohn-Sham orbitals for k-point $\mathbf{k}$, band index ν and spin σ. $|\tilde{\chi}^{\mathbf{R}}_{\mathbf{k}m}\rangle$ is thus a weighted sum of Kohn-Sham orbitals. This sum extends over a given number of Kohn Sham orbitals that can be defined by an index range or alternatively by an energy window $\mathcal{W}$. For a finite $\mathcal{W}$, the orthonormalization of $|\tilde{\chi}^{\mathbf{R}}_{\mathbf{k}m}\rangle$ leads to well defined Wannier functions $|w^{\mathbf{R}}_{\mathbf{k}m}\rangle$, unitarily related to $|\Psi^{\sigma}_{\mathbf{k}\nu}\rangle$: [5]

$$|w^{\mathbf{R}}_{\mathbf{k}m}\rangle = \sum_{\nu\in\mathcal{W}} |\Psi^{\sigma}_{\mathbf{k}\nu}\rangle\langle\Psi^{\sigma}_{\mathbf{k}\nu}|w^{\mathbf{R}}_{\mathbf{k}m}\rangle \tag{29}$$

It is important to notice that the localization of $|w^{\mathbf{R}}_{\mathbf{k}m}\rangle$ will decrease if $\mathcal{W}$ decreases.

Maximally localized Wannier functions are Wannier functions whose extension is minimized[13]. It has the advantage over projected local orbital Wannier functions that it is uniquely defined.

4.1.2 Wannier functions: a pedagogical simplified molecular model

In order to illustrate the localization of Wannier functions, we consider a simple diatomic molecule containing an electropositive atom (V) and an electronegative atom (O). In this model molecule, we consider only one orbital per atom, and for simplification, we assume it is of s symmetry. It can be viewed as a very simple model for $SrVO_3$. The bonding state at ε_1 is the analogue of the O-p like band, whereas the antibonding state at ε_2 is the analogue of the V-d like bands.

We now suppose that the system contains 3 electrons. The V-like band is thus half filled. We use Eq. 28 with $\chi = \phi_V$ to compute Wannier functions for two energy windows:

- If $\mathcal{W} = \{\varepsilon_2\}$, then Eq. 28 contains only one term in the sum: $|\widetilde{\chi}\rangle = |\Psi_2\rangle\langle\Psi_2|\phi_V\rangle = \alpha|\Psi_2\rangle$. After renormalizing $\widetilde{\chi}$, we find that the Wannier function is an extended molecular orbital $|w_V\rangle = |\Psi_2\rangle$ and contains an oxygen contribution. The number of electrons in this orbital is 1.

[5] In the limit of a infinite number of Kohn Sham bands, the projection in Eq. (28) becomes complete and the Wannier functions $|w^{\mathbf{R}}_{\mathbf{k}m}\rangle$ become equivalent to atomic orbitals $|\chi^{\mathbf{R}}_{\mathbf{k}m}\rangle$.

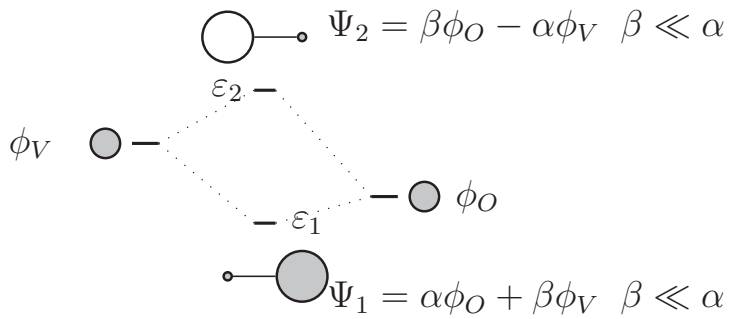

Figure 9: Simple molecular orbital diagram for an diatomic molecule containing an electropositive atom (V) and an electronegative atom (O). It can be viewed as a simple model for $SrVO_3$. In the text, we use this model with 3 electrons: the ϵ_2 level is thus half-filled.

Eigenstates included in the energy window $\mathcal{W}$	$\{\varepsilon_2\}$	$\{\varepsilon_1, \varepsilon_2\}$
Corresponding Wannier function w_V	$\|\Psi_2\rangle$	$\|\phi_V\rangle$
Corresponding number of electrons n_V	1	$2\beta^2 + \alpha^2$

Table 1: Wannier function on vanadium and corresponding numbers of electron in a simple diatomic molecule for two different choices of the energy window.

- If $\mathcal{W} = \{\varepsilon_1, \varepsilon_2\}$, then Eq. 28 contains two terms in the sum. One shows easily that the Wannier function is a localized atomic orbital $|w_V\rangle = |\phi_V\rangle$ and is thus much more localized than in the previous case. The number of electrons in $2\beta^2 + \alpha^2 \neq 1$.

So this simple example illustrates how the localization of the Wannier functions is modified by the choice of energy windows of Kohn Sham bands. A similar illustration in the case of $SrVO_3$ can be seen in [10].

We thus emphasize that the DMFT and the calculation of the effective interactions must be done for the same correlated orbitals. Indeed, the values of effective interactions depends importantly on the localization of Wannier orbitals (see e.g. [14, 15]).

4.2 How to compute the effective coulomb interaction?

When the choice of correlated orbitals is done, the effective interaction for these orbitals has to be computed. There are several ways to compute effective interactions[16, 17, 12]. However, the constrained random phase approximation method[12, 14] (cRPA) is particularly adapted to DFT+DMFT. However, it is not limited to it: indeed, the cRPA method depends crucially on the definition of a many body model[14, 15]. The many-body model is defined by a set of local orbitals together with the interactions among them. A cRPA calculation of a model would require first the definition of a set of local orbitals, and second a consistently calculated screened interaction: it considers that the effective interaction between correlated electrons is the bare interaction screened by all the non correlated electrons. Importantly, thus the value of effective interactions depends crucially[14, 15, 18] on the definition of correlated orbitals discussed above.

We first present the cRPA method, then discuss a self-consistent method to determine U, and finally, we shortly discuss some peculiarity of the PAW implementation.

4.2.1 The cRPA method and the RPA method

We call here χ_0 the non interacting (Kohn-Sham) polarizability of the system. Let's now separate the correlated states (They could be d states but the method is more general and correlated orbitals could

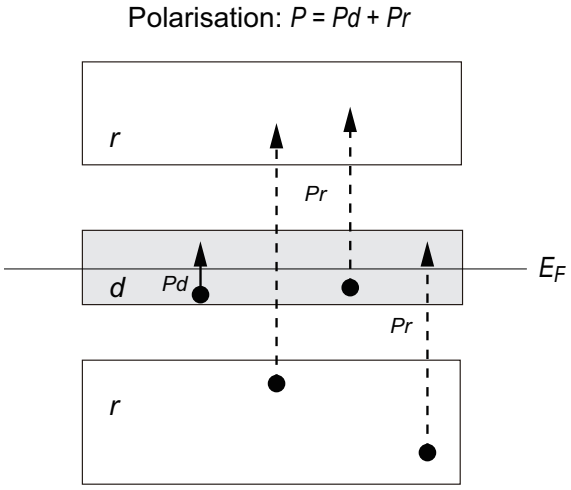

Figure 10: Schematic density of states with the transitions that are involved in the polarizability of correlated electrons $P_d \hat{=} \chi_0^d$ and the other transitions that are involved in $P_r \hat{=} \chi_0^r = P - \chi_0^d$.

gather several orbitals from e.g different atoms) from the rest (r). We thus have[12]:

$$\chi_0 = \chi_0^{\text{correl}} + \chi_0^r \tag{30}$$

thus, we can rewrite the inverse dielectric matrix as:

$$\epsilon^{-1} = \frac{1}{1 - v(\chi_0^{\text{correl}} + \chi_0^r)} \tag{31}$$

We now define the dielectric function due to correlated electrons as

$$\epsilon_{\text{correl}}^{-1} \hat{=} \frac{1}{1 - W_r \chi_0^{\text{correl}}}, \tag{32}$$

the dielectric function of the other electrons as

$$\epsilon_r^{-1} \hat{=} \frac{1}{1 - v\chi_0^r}, \tag{33}$$

and the interaction screened only by the other (r) electrons as:

$$W_r = \frac{v}{1 - v\chi_0^r} \tag{34}$$

With these definitions, one shows that

$$\epsilon_{\text{correl}}^{-1} \epsilon_r^{-1} = ... = \frac{1}{1 - v\chi_0^r - v\chi_0^{\text{correl}}} = \frac{1}{1 - v\chi_0} = \epsilon^{-1} \tag{35}$$

Thus, we have

$$W \hat{=} \epsilon^{-1} v = \epsilon_{\text{correl}}^{-1} \epsilon_r^{-1} v \tag{36}$$

We can interpret this result[12]: The fully screened RPA interaction is the combination of two screening processes. First, the bare interaction is screened by non-correlated electrons (r), and it gives rises to a screened interaction W_r. Secondly the screening of this interaction by correlated electrons recovers the fully screened interaction.

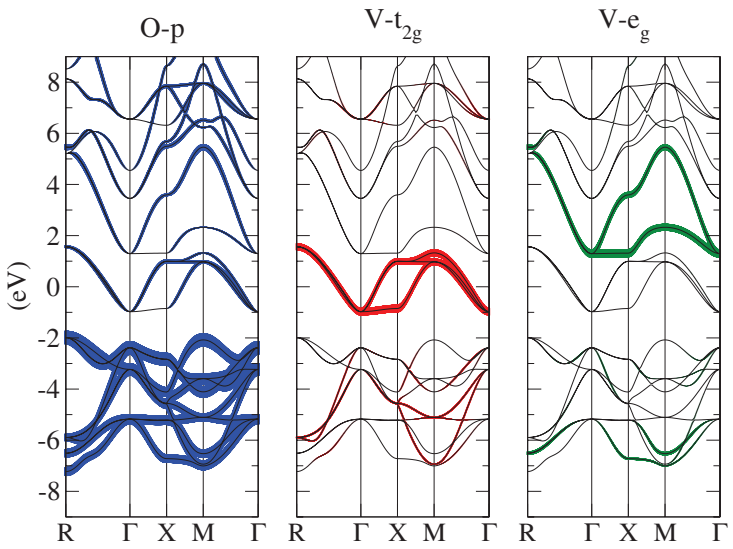

Figure 11: "Fatbands" of $SrVO_3$, corresponding to the O-p, V-t_{2g}, and V-e_g like bands [21]. Between -8 eV and -2 eV, bands are mainly Op-like. Then, there are 3 bands of t_{2g} character that cross the Fermi level, and finally 2 bands of e_g character. If Wannier correlated orbitals are constructed only with V-t_{2g}-like bands, then, the cRPA interactions can be computed by removing transitions inside the three isolated V-t_{2g}-like bands.

The main idea of cRPA is to use this separation of screening processes. The screened interaction W_r can be computed explicitly, using the equation written above, which is valid for electrons interacting only with the Hartree potential (it could be generalized to electrons interacting with the LDA potential, by adding the LDA exchange and correlation kernel). Removing screening by correlated electrons is easy in cases where correlated orbitals are unitarily related to an isolated set of bands (see Fig. 10). In other cases, several disentanglements[19] or weighting schemes have been proposed[20]. The weighting scheme of [20] lowers the contribution of a given transition, as a function of the weight of correlated orbitals on the bands involved in the transition.

Then the interaction in the basis of correlated orbitals is computed with:

$$U_{1234}(w) = \langle w_1 w_2 | W_r(w) | w_3 w_4 \rangle \tag{37}$$

Finally, the screening by correlated electrons is explicitly taken into account by solving exactly correlations with the interaction U_{1234} by a dedicated method (e.g. DMFT).

4.2.2 Many body models

We now briefly discuss different kind of models as discussed in Ref.[14, 15] in the case of $SrVO_3$, which is a test systems for various methods[22, 10, 14]. $SrVO_3$ is a correlated metal with one electron in the Vt_{2g}-like band (see discussion in Fig. 11).

model (screening-orbital)	v	U
$d-d$	15.0	2.8
$dp-dp$	19.4	10.1

Table 2: Bare (v), and cRPA (U) Coulomb interactions for $SrVO_3$ computed for different models. Results are from [18] and similar results are obtained in Refs. [14] and [15].

- d model: The model is built from the Vd-like bands only: Wannier functions are build from Vd-like bands and transitions among the Vd-like bands define χ^{correl}.
- dp model: The model is built from the Vd-like and Od-like bands. Wannier functions are build from Vd-like bands and Op-like bands and transitions among these bands define χ^{correl}. In this case, effective interactions U_{dd}, U_{pp} and U_{pd} can be computed and used in a calculation using explicitly all these interactions.

The value of U depends largely on the model[14]. It is thus especially important to accompany the value of U with the definition of the model used.

4.3 The DFT+DMFT loops

In a first step, we are going to write the expression of the lattice Green's function for the solid with a local self-energy. The self-energy will later be the DMFT self-energy.

4.3.1 The lattice Green's function

In comparison to the case of the one band Hubbard model, things are more complicated because

- The number of correlated orbitals is larger (10 for d elements)
- The number of bands in the system is large, and larger that the number of correlated orbitals because some orbitals are not correlated. For example, in Iron, the $3d$ orbitals are correlated but the $4s$ are not. However, $4s$ and $3s$ states are strongly mixed in the DFT/LDA density of states.

We are going to express all quantities (G, Σ) in the Kohn Sham wavefunctions basis because the DFT Hamiltonian has a simple expression in this basis:

$$H_{\text{LDA}} = \sum_{n\mathbf{k}} |\Psi_{\mathbf{k}n}\rangle \epsilon_{n\mathbf{k}} \langle \Psi_{\mathbf{k}n}| \tag{38}$$

The self energy in DMFT is local and is computed in a local basis, thus the self energy operator is a sum of identical self-energies on each correlated sites (m and m' are quantum numbers of the projection of the angular momentum).

$$\Sigma = \sum_{mm'\mathbf{T}_i} |\chi_{\mathbf{T}_i m}\rangle \Sigma_{m,m'}(\omega) \langle \chi_{\mathbf{T}_i m'}| \tag{39}$$

We can define the Bloch transform of the localized functions $\chi_{\mathbf{T}_i m}$ as before as

$$|\chi_{\mathbf{T}_i m}\rangle = \frac{1}{\sqrt{N}} \sum_{\mathbf{k}} |\chi_{\mathbf{k}m}\rangle \mathrm{e}^{-i\mathbf{k}\mathbf{T}_i}. \tag{40}$$

Thus by replacing the last equation in Eq. 39, we have:

$$\Sigma = \sum_{mm'\mathbf{k}} |\chi_{\mathbf{k}m}\rangle \Sigma_{m,m'}(\omega) \langle \chi_{\mathbf{k}m'}|. \tag{41}$$

It can be expressed in the Kohn Sham basis directly using the fact that $\langle \Psi_{\mathbf{k}n} | \chi_{\mathbf{k}'m} \rangle$ is zero if $\mathbf{k}$ and $\mathbf{k}'$ are different,

$$\Sigma_{nn'}(\mathbf{k}, \omega) = \sum_{m,m'} \langle \Psi_{\mathbf{k}n} | \chi_{\mathbf{k}m} \rangle \Sigma_{mm'}(\omega) \langle \chi_{\mathbf{k}m'} | \Psi_{\mathbf{k}n'} \rangle \tag{42}$$

In order to avoid a double counting of the correlation for correlated orbitals, the self-energy has to contain a so called "double counting part" which should cancel the DFT/LDA Hartree and exchange correlation potential for the correlated electrons

$$\Sigma = \Sigma_{\mathrm{DMFT}} - \Sigma_{\mathrm{DC}}. \tag{43}$$

The Green's function will obey the usual equation of motion:

$$(\omega I - H - \Sigma)G = I. \tag{44}$$

Thus the Green's function is

$$G_{nn'}(\mathbf{k},\omega) = \left[\omega I - H(\mathbf{k}) - \Sigma(\mathbf{k},\omega)\right]^{-1}\big|_{nn'}, \tag{45}$$

where $H(\mathbf{k})$ is a diagonal matrix containing the Kohn Sham eigenvalues and $\Sigma(\mathbf{k},\omega)$ is non diagonal (see above).

The local Green's function is simply:

$$G^{\mathrm{loc}}_{mm'}(\omega) = \sum_{\mathbf{k}} \langle \chi_{\mathbf{k}m} | \Psi_{\mathbf{k}n} \rangle G_{nn'}(\mathbf{k},\omega) \langle \Psi_{\mathbf{k}n'} | \chi_{\mathbf{k}m'} \rangle \tag{46}$$

This equation is the generalisation of Eq. 21.

4.3.2 The Self-Consistency Condition

The DMFT self-consistency relation equals the local Green's function and the Green's function of the Anderson model:

$$G^{\mathrm{loc}}_{mm'}(\omega) = G^{\mathrm{Anderson}}_{mm'}(\omega) \tag{47}$$

where

$$G^{\mathrm{Anderson}}_{mm'}(\omega) = \left[\omega I - E_0 - \Delta(\omega) - \Sigma(\omega)\right]^{-1}\big|_{mm'} \tag{48}$$

E_0 is a diagonal matrix with the levels of correlated orbitals in the (multiorbital) Anderson model, Σ and Δ are the self-energy and hybridization matrices in the correlated orbital basis. E_0 and Δ are obtained from the self-consistency condition.

4.3.3 The Anderson impurity model

E_0, Δ and U, J defines the Anderson model. The solution of the Anderson model gives the local self energy, which is used again to compute the lattice Green's function (Eq. 45).

4.3.4 The DFT loop

The density can be obtained from the full Green's function using:

$$n(\mathbf{r}) = -i \sum_{n,\mathbf{k}} \Psi_{\mathbf{k}n}(\mathbf{r}) G_{nn'}(\mathbf{k}, t - t' = 0^-) \Psi_{\mathbf{k}n'}(\mathbf{r}) \tag{49}$$

and is used to reconstruct the Kohn Sham hamiltonian (a functional of the density) and thus the eigenvalues. The scheme is summarized on Fig. 12.

5 Conclusion

In these notes, we have first shown that the Hubbard model is a model for localisation/delocalisation transitions. Then we have presented the mapping to the Anderson model, and finally the DMFT and DFT+DMFT equations. The next lecture shows a more formal derivation based on functionals. For interested readers, the ABINIT code proposes online hands-on tutorials about "how to compute U using cRPA", and "the DFT+DMFT method" (see www.abinit.org/tutorials).

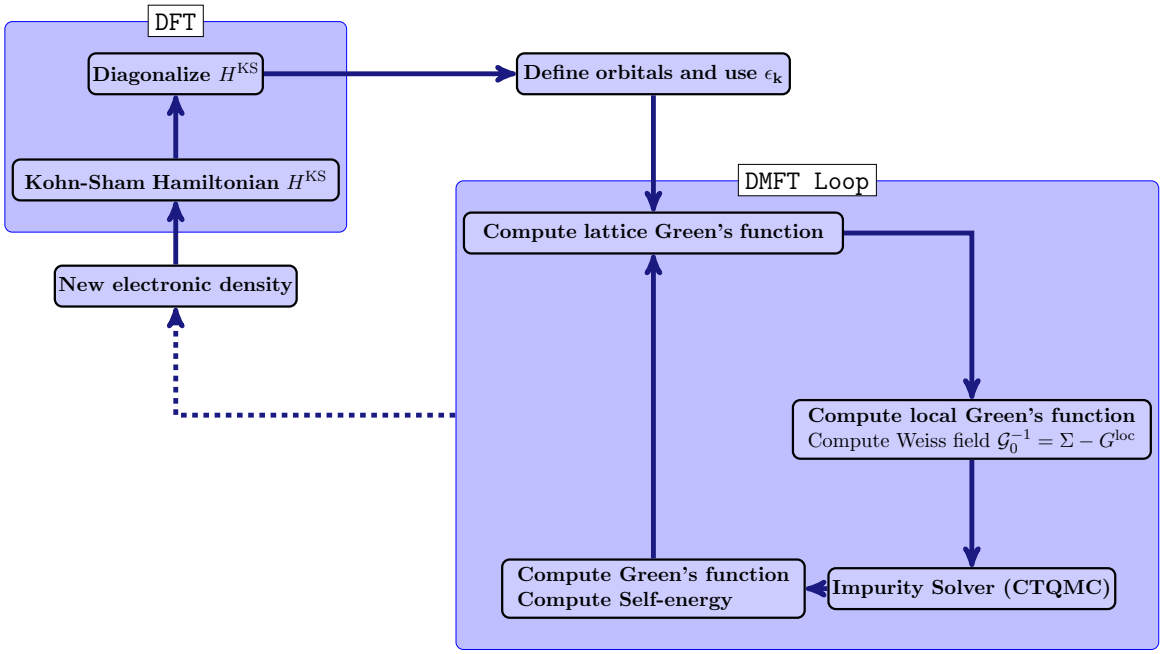

Figure 12: Scheme of the DFT+DMFT loops. $\mathcal{G}_0$ is the non interacting Green's function of the Anderson model and is linked to the hybridization by $\mathcal{G}_0^{-1} = [\omega I - E_0 - \Delta(\omega)]$. The Dyson Equation is $\mathcal{G}_0^{-1} - G^{-1} = \Sigma$.

References

[1] Antoine Georges, Gabriel Kotliar, Werner Krauth, and Marcelo J. Rozenberg. Dynamical mean-field theory of strongly correlated fermion systems and the limit of infinite dimensions. *Rev. Mod. Phys.*, 68:13–125, Jan 1996.

[2] G. Kotliar, S. Y. Savrasov, K. Haule, V. S. Oudovenko, O. Parcollet, and C. A. Marianetti. Electronic structure calculations with dynamical mean-field theory. *Rev. Mod. Phys.*, 78(3):865–951, August 2006.

[3] Antoine Georges. Strongly correlated electron materials: Dynamical mean-field theory and electronic structure. *AIP Conf. Proc.*, 715(1):3–74, August 2004.

[4] S.S. Hecker. The magic of plutonium: 5f electrons and phase instability. *Metallurgical and Materials Transactions A*, 35(8):2207–2222, 2004.

[5] A.K. McMahan, C. Huscroft, R.T. Scalettar, and E.L. Pollock. Volume-collapse transitions in the rare earth metals. *Journal of Computer-Aided Materials Design*, 5(2):131–162, 1998.

[6] P. W. Anderson. Localized magnetic states in metals. *Phys. Rev.*, 124:41–53, Oct 1961.

[7] P Fulde. Introduction to the theory of heavy fermions. *Journal of Physics F: Metal Physics*, 18(4):601, 1988.

[8] Gabriel Kotliar and Dieter Vollhardt. Strongly correlated materials: Insights from dynamical mean-field theory. *Phys. Today*, 57(3):53–59, March 2004.

[9] V. I. Anisimov, D. E. Kondakov, A. V. Kozhevnikov, I. A. Nekrasov, Z. V. Pchelkina, J. W. Allen, S.-K. Mo, H.-D. Kim, P. Metcalf, S. Suga, A. Sekiyama, G. Keller, I. Leonov, X. Ren, and D. Vollhardt. Full orbital calculation scheme for materials with strongly correlated electrons. *Phys. Rev. B*, 71:125119, Mar 2005.

[10] F. Lechermann, A. Georges, A. Poteryaev, S. Biermann, M. Posternak, A. Yamasaki, and O. K. Andersen. Dynamical mean-field theory using wannier functions: A flexible route to electronic structure calculations of strongly correlated materials. *Phys. Rev. B*, 74:125120, Sep 2006.

[11] B. Amadon, F. Lechermann, A. Georges, F. Jollet, T. O. Wehling, and A. I. Lichtenstein. Plane-wave based electronic structure calculations for correlated materials using dynamical mean-field theory and projected local orbitals. *Phys. Rev. B*, 77(20):205112–, May 2008.

[12] F. Aryasetiawan, M. Imada, A. Georges, G. Kotliar, S. Biermann, and A. I. Lichtenstein. Frequency-dependent local interactions and low-energy effective models from electronic structure calculations. *Phys. Rev. B*, 70(19):195104–, November 2004.

[13] Nicola Marzari and David Vanderbilt. Maximally localized generalized wannier functions for composite energy bands. *Phys. Rev. B*, 56:12847–12865, Nov 1997.

[14] Loïg Vaugier, Hong Jiang, and Silke Biermann. Hubbard U and hund exchange J in transition metal oxides: Screening versus localization trends from constrained random phase approximation. *Phys. Rev. B*, 86(16):165105–, October 2012.

[15] R. Sakuma and F. Aryasetiawan. First-principles calculations of dynamical screened interactions for the transition metal oxides MO (M=Mn, Fe, Co, Ni). *Phys. Rev. B*, 87(16):165118–, April 2013.

[16] V. I. Anisimov and O. Gunnarsson. Density-functional calculation of effective coulomb interactions in metals. *Phys. Rev. B*, 43(10):7570–7574, April 1991.

[17] Matteo Cococcioni and Stefano de Gironcoli. Linear response approach to the calculation of the effective interaction parameters in the lda+u method. *Phys. Rev. B*, 71(3):035105–, January 2005.

[18] Bernard Amadon, Thomas Applencourt, and Fabien Bruneval. Screened coulomb interaction calculations: cRPA implementation and applications to dynamical screening and self-consistency in uranium dioxide and cerium. *Phys. Rev. B*, 89:125110, Mar 2014.

[19] Takashi Miyake, Ferdi Aryasetiawan, and Masatoshi Imada. Ab initio procedure for constructing effective models of correlated materials with entangled band structure. *Phys. Rev. B*, 80(15):155134–, October 2009.

[20] Bi-Ching Shih, Yubo Zhang, Wenqing Zhang, and Peihong Zhang. Screened coulomb interaction of localized electrons in solids from first principles. *Phys. Rev. B*, 85(4):045132–, January 2012.

[21] Eva Pavarini, Erik Koch, Dieter Vollhardt, and Alexander Lichtenstein, editors. *Lecture notes on DFT+DMFT*. 2011.

[22] E. Pavarini, S. Biermann, A. Poteryaev, A. I. Lichtenstein, A. Georges, and O. K. Andersen. Mott transition and suppression of orbital fluctuations in orthorhombic $3d^1$ perovskites. *Phys. Rev. Lett.*, 92:176403, Apr 2004.